Excited State Energy Transfer Pathways in Photosynthetic Reaction Centers. 3. Ultrafast Emission from the Monomeric Bacteriochlorophylls

Brett A. King, Tim B. McAnaney, Alex deWinter, and Steven G. Boxer*

Department of Chemistry, Stanford University, Stanford, California 94305-5080

Received: May 11, 2000; In Final Form: June 29, 2000

Ultrafast singlet excited state energy transfer occurs from the monomeric bacteriopheophytin (H) and bacteriochlorophyll (B) chromophores to the primary electron donor or special pair (P) in bacterial photosynthetic reaction centers. Because of rapid quenching of the singlet excited state of B by energy transfer to P, ^{1}B emission has not previously been observed in functional reaction centers. Using fluorescence upconversion, spontaneous fluorescence associated with the monomeric bacteriochlorophylls is observed for excitation of the monomeric bacteriochlorophylls and bacteriopheophytins at 85 K. The decay kinetics of the fluorescence match the kinetics of the rise of emission from ^{1}P, the ultimate acceptor of singlet energy. Together with measurements of the time-resolved fluorescence anisotropy, the data suggest that ^{1}B is populated in the energy transfer pathway from ^{1}H to P. By exciting H in wild-type and in the reaction center mutant M182HL, where contributions from the chromophores in the B sites on the L and M sides are spectrally resolved, the amplitudes of the kinetic traces at several wavelengths between 790 and 825 nm can be used to construct the time-resolved emission spectrum of ^{1}B. The Stokes shift of the accessory bacteriochlorophylls in wild-type on the femtosecond time scale is close to zero, while for the monomeric bacteriopheophytin in the B_M binding site in the M182HL mutant, the Stokes shift is less than 100 cm^{-1}. These results have significant implications for the mechanism of ultrafast energy transfer in the reaction center.

The bacterial photosynthetic reaction center (RC) is responsible for the initial light-driven charge separation events in photosynthesis. Light energy absorbed by antenna complexes is funneled to the special pair in the RC, and ^{1}P transfers an electron to an electron acceptor, rapidly trapping the excitation energy in a transient charge-separated species. In isolated RCs, excitation of the special pair can be achieved by rapid singlet excited state energy transfer from the monomeric bacteriopheophytins and bacteriochlorophylls.[1−3] A schematic diagram illustrating the arrangement of the chromophores that are relevant to both the energy and electron-transfer processes is shown in Figure 1 (top panel) based on the X-ray structure,[4] and a putative singlet excitation energy transfer scheme paralleling the structure is shown in Figure 1 (bottom panel). The chromophores labeled B_L and B_M are monomeric bacteriochlorophylls on the functional and nonfunctional sides, respectively, of the RC; the chromophores labeled H_L and H_M are monomeric bacteriopheophytins on the functional and nonfunctional sides, respectively. Functional is used here to denote the electron-transfer process $^1P \rightarrow P^+H_L^-$ which is found to occur almost exclusively in wild-type RCs at all temperatures, despite the structural symmetry of the RC that suggests that $^1P \rightarrow P^+H_M^-$ might be equally likely to occur.

It is possible to study the rate of singlet energy transfer from the B and H chromophores to P by femtosecond transient absorption spectroscopy or by measuring the rise of ^{1}P fluorescence using fluorescence upconversion. In earlier work, our group and others showed that energy transfer from $^1B \rightarrow P$ and from $^1H \rightarrow P$ is very fast.[1−3,5] By using the mutant M214LH[6,7] (the β mutant, where a bacteriochlorophyll, β_L, replaces H_L), in which selective excitation of β_L or H_M is possible, we showed that the rates of energy transfer to P along the L and M branches are comparable.[5] We also demonstrated that upon removing the central Mg^{2+} ion from one of the

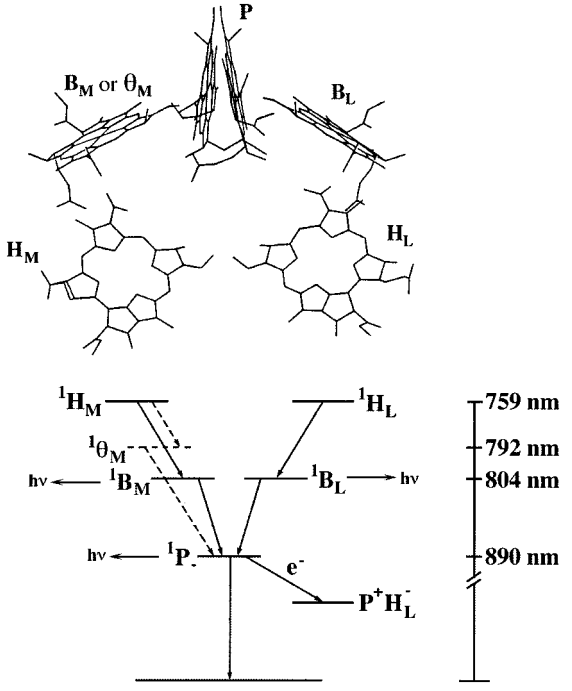

Figure 1. (Top panel) schematic diagram of the chromophores involved in the energy and electron-transfer processes of isolated *Rb. sphaeroides* photosynthetic reaction centers taken from the X-ray structure.[4] (Bottom panel) schematic energy level diagram taken from the absorption spectrum at 77 K illustrating possible energy transfer pathways paralleling the structure in the top panel.

* Corresponding author. Phone: (650) 723-4482; Sboxer@Stanford.edu.

10.1021/jp001745u CCC: $19.00
Published on Web 08/24/2000

bacteriochlorophylls of the special pair dimer in the heterodimer mutant, M202HL, energy transfer from $^1B_L \rightarrow P$ is slowed relative to $^1B_M \rightarrow P$.[8,9]

Singlet energy transfer from the monomeric bacteriopheophytins to the special pair in wild-type RCs requires more time than from the monomeric bacteriochlorophylls.[5] This is not surprising since H_L and H_M are considerably further from P than B_L and B_M (center-to-center distances ~17 Å for H vs ~10 Å for B). The greater distance, along with the presumed negligible spectral overlap between ^1H emission and P absorption, makes direct energy transfer between ^1H and P on this time scale unlikely. A more reasonable model is that energy transfer occurs sequentially, first from ^1H to B and then from ^1B to P. Given the independently measured rate constants from $^1H \rightarrow P$ and from $^1B \rightarrow P$, the rate constant from $^1H \rightarrow B$ should be comparable to that from $^1B \rightarrow P$ (see Appendix).[5] If ^1B is a real intermediate in the energy transfer pathway, then a detectable transient excited state population of ^1B would be present about 100 fs after excitation of H. Alternatively, $^1H \rightarrow P$ energy transfer could involve ^1B as a virtual intermediate; that is, energy transfer could occur by a superexchange mechanism. In this case, it would not be possible to directly detect the ^1B population. In the following, we use fluorescence upconversion to measure the excited state dynamics of ^1B following excitation of the H or B chromophores in *Rhodobacter sphaeroides* RCs. In addition, the time-resolved emission spectrum of ^1B is obtained following excitation of H, giving information on the Stokes shift of the monomeric bacteriochlorophylls in situ. This is relevant to the underlying mechanism of ultrafast $^1B \rightarrow P$ energy transfer and our hypothesis that comparison of the rates of $^1B_L \rightarrow P$ vs $^1B_M \rightarrow P$ energy transfer may probe differences in the electronic interactions on the L vs M sides of the RC that are relevant to unidirectional electron transfer.

Experimental Section

The low-temperature fluorescence upconversion spectrometer has been described in detail previously, along with methods for measuring fluorescence anisotropies and analyzing the data.[10] Briefly, samples were excited using a mode-locked Ti:sapphire laser (Spectra Physics Tsunami) pumped by 6−10 W (all lines) from an argon-ion laser (Spectra Physics model 2080). For experiments exciting at 804.5 nm, the pulse widths were ~80 fs with a time−bandwidth product typically less than 0.43. The maximum pulse width used in these experiments was ~110 fs when exciting at 760 nm. Samples were excited at the magic angle with respect to the gate beam used for fluorescence upconversion with <250 pJ of energy per pulse. Decays were obtained with a delay line step size of 21 fs/point. Low temperature was achieved by using a miniature Joule-Thompson refrigerator (MMR Technologies, Mountain View, CA) and a very thin sample geometry. For wild-type RCs, fluorescence rise and decay curves were measured at 800, 804.9, 807.4, 810, 812.4, 814.9, 820.3, and 825 nm for excitation at 760 nm on the same sample under the same conditions (same excitation power and same monochromator slit width). For the M182HL mutant, fluorescence rise and decay curves were measured at 789.8, 794.8, 797.3, 799.9, 802.4, 804.8, 807.2, 809.8, 814.8, and 819.9 nm for excitation at 750 nm. Each scan required approximately 10 min, after which the monochromator detection wavelength was changed, the phase-matching angle of the BBO crystal was adjusted (by no more than 3° over the wavelength ranges above), and the interference filter in front of the monochromator was angle-tuned for maximum throughput of the detection wavelength. The same interference filter was used for all detection wavelengths. The initial amplitudes (or the integrated intensities) of the fluorescence decay curves were multiplied by a correction factor to account for the relative transmittance of the interference filter at different detection wavelengths, which was measured separately in a spectrophotometer. The range of angles over which the interference filter was rotated was small enough that refraction of the beam resulted in a less than 1% change in transmittance, which is small enough to be neglected. Over the wavelength range of these experiments, the fluorescence upconversion efficiency of the nonlinear crystal changes by no more than 3%, which is small enough to be neglected. The corrected initial amplitudes were then plotted versus wavelength to map out the time-resolved fluorescence spectra.

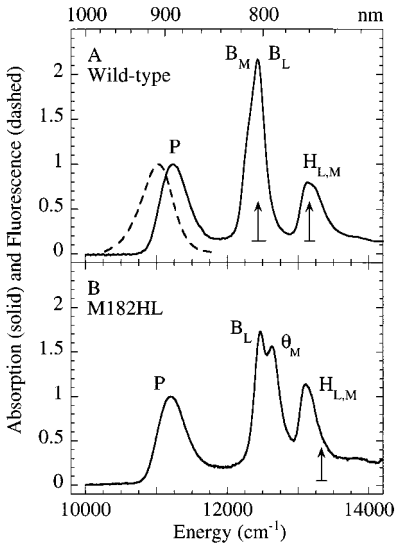

Figure 2. Absorption spectra (solid) and fluorescence spectrum (dashed) in the Q_y region at 77 K for Q-reduced *Rb. sphaeroides* wild-type (A) and mutant M182HL in which a bacteriopheophytin *a*, labeled θ_M, replaces a bacteriochlorophyll in the B_M binding site (B). The vertical arrows illustrate wavelengths used for excitation and the horizontal bars indicate the excitation widths.

Poly-His tagged wild-type[11] (WT) and M182HL mutant *Rb. sphaeroides* cells were grown semi-aerobically, the RCs were isolated, and the detergent was exchanged for Triton X-100. The gene coding for the M182HL mutation was generously provided by Professor Neal Woodbury; this was then ligated into the poly-His background for ease of isolation.[11] His182 is the ligand for the central Mg^{2+} ion in the bacteriochlorophyll that occupies the B_M binding site. By replacing this His with a nonligating Leu residue, the Mg^{2+} ion is lost, and a bacteriopheophytin *a* is found to occupy the B_M binding site,[12] as is readily seen in the absorption spectrum (Figure 2B); this chromophore is denoted θ_M. The M182HL and WT RCs contain carotenoid, which is important for experiments using relatively high repetition rate excitation.[13] All samples were dissolved in 1/1 (v/v) glycerol/buffer (10 mM Tris, 0.1% Triton X-100, pH 8.0) solution, and quinone Q_A was reduced using sodium dithionite. The RCs were concentrated in order to achieve a sufficient optical density in the 25−50 μm path length cell, typically 0.1−0.2 at 800 nm.

Results

Time-Resolved Fluorescence from ^1B. For WT RCs at 85 K, the time-resolved fluorescence at 850 nm for excitation at

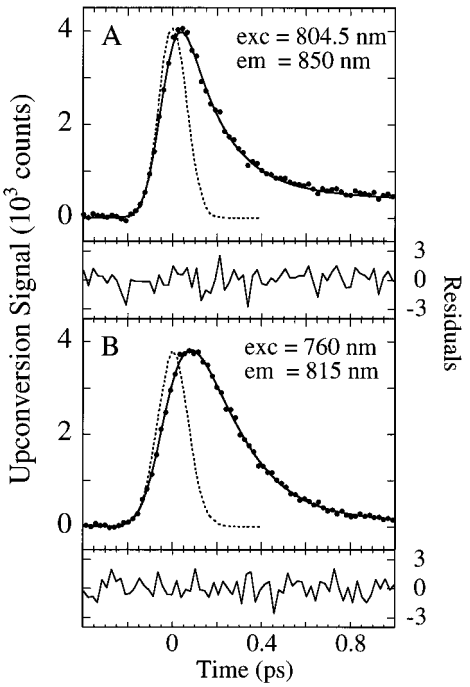

Figure 3. Spontaneous fluorescence (circles) at 85 K from wild-type RCs in the B band region. Panel A shows the emission measured at 850 nm following excitation in the B band at 804.5 nm. Panel B shows the emission measured at 815 nm following excitation in the H band at 760 nm. Fits to the data are shown (solid line, see Table 1 for lifetimes) and the cross correlations (dashed) are overlaid. The residuals of the fits are displayed below the data.

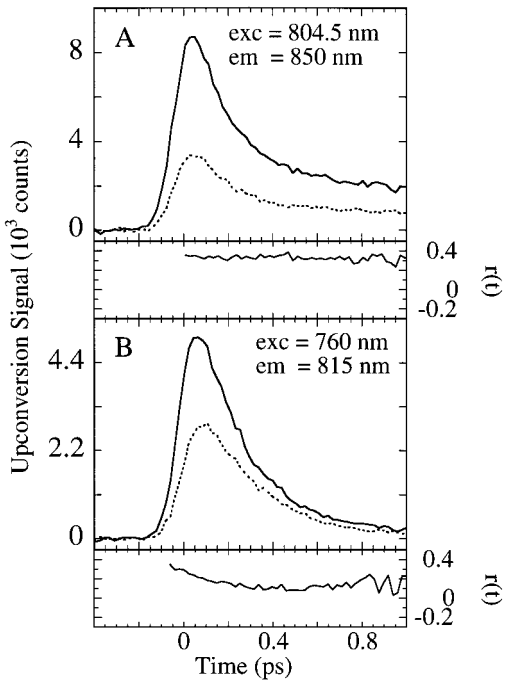

Figure 4. Fluorescence decays for parallel (solid lines) and perpendicular (dashed lines) polarized excitation and associated anisotropy, $r(t)$, of wild-type RCs at 85 K for excitation at 804.5 nm and emission at 850 nm (A) and for excitation at 760 nm and emission at 815 nm (B).

804.5 nm (both B chromophores) and at 815 nm for excitation at 760 nm (both H chromophores) are shown in Figure 3. The time-resolved anisotropy for these wavelength pairs is shown in Figure 4. For excitation at 804.5 nm, it is difficult to detect nearer to the excitation wavelength than 850 nm due to the background produced by the frequency-doubled gate beam at shorter detection wavelengths. For the same reason, 800 nm is our limit of detection for excitation at 760 nm. When H is excited at 760 nm, a negative amplitude component is necessary to fit the rise at 815 nm, indicative of energy transfer to the emitting state. The lifetime of the rise is 85 ± 17 fs, shorter than the 150 fs cross correlation. The decay of the emission between 800 and 825 nm is essentially monoexponential with a lifetime of 199 ± 16 fs associated with 99% of the amplitude and a minor component with about 1% of the amplitude whose lifetime is several picoseconds. The time-resolved emission anisotropy decays initially and stabilizes after ~200 fs at a value of 0.102 ± 0.022, corresponding to an angle of 44.8 ± 1.9° between the H absorption transition dipole moment and the emission transition dipole moment of the emitting species. For excitation at 804.5 nm and emission at 850 nm, the fit requires two exponential components for the decay (no rise component is necessary), the lifetimes (and amplitudes) of which are 160 ± 12 fs (89 ± 2%) and 2.8 ± 0.2 ps (11 ± 2%). The latter component is most likely a small contribution from ^{1}P emission. The anisotropy of the major component is 0.350 ± 0.014, corresponding to an angle of 16.8 ± 2.0°. These results are summarized in Table 1.

Emission around the B band is also observed for excitation of the monomeric bacteriopheophytins at 760 nm in the M182HL mutant (data not shown). The kinetics are similar to those for WT; the lifetime of the major decay component in the mutant is 227 ± 22 fs (see Table 1).

TABLE 1: Rise and Decay Times for the Major Components of the Spontaneous Fluorescence from ^{1}B and ^{1}P in Wild Type and M182HL Mutant Reaction Centers for Excitation at 760 nm and at 804 nm at 85 K

reaction center	λ_{exc} (nm)	λ_{em} (nm)	τ_{rise} (fs)	τ_{decay} (fs)	anisotropy r
wild type	804.5	850	prompt[a]	160 ± 12	0.350 ± 0.014
		940	163 ± 54[b]	1130 ± 40	0.241 ± 0.003
	760	815	85 ± 17	199 ± 16	0.102 ± 0.022
		920[c]	178 ± 38	97 ± 43	−0.015[b]
				1210 ± 47	
M182HL	804	920	145 ±11	1300 ± 106	
	760	815	93 ± 25	227 ± 22	
		920[c]	157 ± 16	112 ± 26	
				1220 ± 90	

[a] Faster than can be resolved with the 120 fs (fwhm) cross correlation. [b] Value from Stanley et al.[5] [c] The two femtosecond components reflect the two energy transfer steps ^{1}H → B (appears in the decay) and ^{1}B → P (appears in the rise), while the picosecond decay component is the same one observed for direct excitation of P. See Appendix for further discussion.

Time-Resolved Emission Spectrum of ^{1}B. The corrected relative amplitudes of the fluorescence decay curves (see Experimental Section) measured at wavelengths between 800 and 825 nm for excitation of WT RCs at 760 nm (85 K) are shown in Figure 5A. This time-resolved emission spectrum is the average of three data sets from two samples. Comparison of data points taken in 2.5 nm steps around the peak of the B band with the absorption spectrum, whose maximum is at 804.5 nm at 77 K, indicates that the emission Stokes shift on the femtosecond time scale is close to 0 cm^{-1} assuming the emission is from ^{1}B (see below). For 750 nm excitation of M182HL RCs at 85 K, the corrected relative amplitudes of the fluorescence decay curves at wavelengths between 790 and 820 nm are shown in Figure 5B. The results are the average of five data sets from two samples. The emission is relatively flat between 792 and

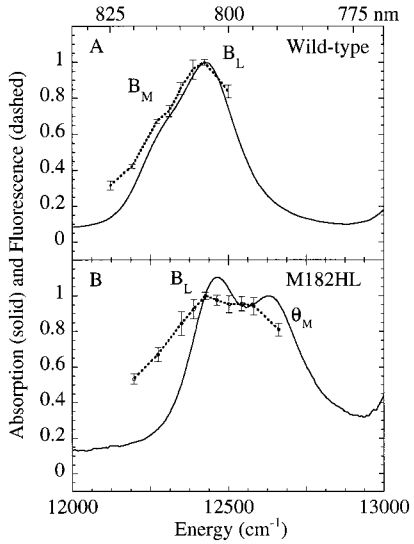

Figure 5. Absorption in the Q_y region (solid, 77 K) and time-resolved emission (dashed, 85 K) spectra of the B band for Q-reduced wild-type (A) and M182HL (B) RCs. The excitation wavelengths for the time-resolved emission spectra were 760 nm in wild-type and 750 nm in the M182HL mutant. The time-resolved emission spectra were constructed from corrected amplitudes of the fluorescence decays collected at 85 K. The error bars show the standard deviation of three data sets for WT and five data sets for the M182HL mutant.

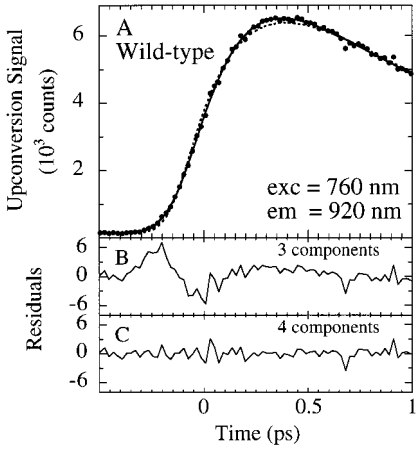

Figure 6. Spontaneous fluorescence from ^{1}P at 920 nm in wild-type RCs following excitation at 760 nm (A). Two fits are shown: a three-component fit (dashed) and four-component fit (solid). The residuals of the three-component fit (B) and four-component fit (C) are shown in the lower panels (see text and Appendix).

800 nm and peaks at 805 nm. The corresponding Stokes shifts relative to the absorption peak positions of B_L and θ_M are ~35 and 70−100 cm^{-1}, respectively. For both WT and M182HL, the decay lifetimes are the same within experimental error at all of the emission wavelengths used to construct the time-resolved emission spectra (data not shown).

Time-Resolved Emission from ^{1}P. The lifetimes of the rise of emission from ^{1}P in WT and the M182HL mutant are summarized in Table 1. For the M182HL mutant (data not shown), the lifetimes of the rise of emission from ^{1}P measured at 920 nm for excitation of B or H are comparable to the values we have previously reported for WT. Figure 6A shows the rise and initial decay of ^{1}P emission for excitation of H in WT along with fits using three and four exponential components. Fitting the data with four exponential components yields a rise lifetime (and amplitude) of 178 ± 38 fs (−98 ± 2%) and decay components with lifetimes (and amplitudes) of 97 ± 43 fs (59 ± 34%), 1.21 ± 0.04 ps (39 ± 32%), and 14 ± 2 ps (3 ± 2%).[14] The latter two decay times and their relative amplitudes agree with the values for ^{1}P decay when P is excited directly.[10] In previous work,[5] spontaneous fluorescence signals were fit to a sum of three exponentials, one having a negative amplitude to account for energy transfer and two having a positive amplitude to account for the excited state decay. For energy transfer from ^{1}B to P, both a reduced χ^2 value typically less than 1.2 and unstructured residuals [(fit − data)/$\sqrt{}$fit)] indicate that the model accounts for the data. For energy transfer from ^{1}H to P, which involves two-step energy transfer ^{1}H → B followed by ^{1}B → P, fitting the data with three exponential components is expected and found to be inadequate. With a three-component fit, the reduced χ^2 value is typically greater than 1.4 and the residuals are structured around the rise and peak of the fluorescence signal (Figure 6B). As discussed in detail in the Appendix, in the two-step energy transfer mechanism, the rate constants for *both* energy transfer components should appear in the dynamics of ^{1}P. This and the high signal-to-noise of the data justify the addition of one more exponential component to the fit. Unstructured residuals are obtained when a sum of four exponential components is used (Figure 6C and Appendix).

Discussion

Energy Transfer from ^{1}H and ^{1}B to P and ^{1}B Emission. The observation of fluorescence between 800 and 850 nm in functional RCs is a significant result, as it has not been previously observed, in either steady state or time-resolved spectra. Using fluorescence upconversion, emission is observed at 850 nm for excitation in the B band at 804.5 nm in WT RCs at 85 K (Figure 3A); the lifetime of the dominant component of the decay is 160 ± 12 fs. Energy transfer from ^{1}B to P as measured by the rise of emission from ^{1}P at 940 nm for 804 nm excitation is 163 ± 54 fs.[5] That the decay of emission at 850 nm matches the rise of emission from ^{1}P suggests that the excited state probed at 850 nm transfers energy to P.[15] Emission between 800 and 850 nm is observed for excitation in the H band at 760 nm in WT RCs at 85 K (Figure 3B shows emission at 815 nm). The emitting state is populated with a lifetime of 85 ± 17 fs (^{1}H → B) and decays with a lifetime of 199 ± 16 fs (^{1}B → P). These energy transfer components appear in the dynamics of ^{1}P measured at 920 nm (see Appendix), giving rise and decay lifetimes of 178 ± 38 and 97 ± 43 fs, respectively, in addition to the 1.2 and 14 ps components associated with electron transfer from ^{1}P (the picosecond components are the same as those observed for direct excitation of P). In the two-step energy transfer mechanism, the rate constants for each energy transfer step should appear in the kinetics of both the intermediate and final states, providing an internal check on the mechanism. That the kinetic components of the excited state probed between 800 and 850 nm for excitation of $H_{L,M}$ are also observed in the rise and decay of emission from ^{1}P suggests that the excited state transfers energy to P. Together with the time-resolved anisotropy discussed below, the kinetics support the assignment of fluorescence between 800 and 850 nm to ^{1}B.

The measured anisotropy exciting B at 804.5 nm and detecting emission at 850 nm is 0.350 ± 0.014 (Figure 4A). An anisotropy of 0.326 is observed in the steady state for bacteriochlorophyll *a* monomers in castor oil at room temperature.[16] The agreement between these measurements is consistent with excitation and emission from the same chromophore and suggests that the

excited state probed at 850 nm is ^{1}B. For excitation of H at 760 nm and emission at 815 nm, the time-resolved anisotropy is 0.102 ± 0.022, corresponding to an angle of 44.8 ± 1.9° between the H absorption and the emission transition dipole moment(s) of the emitting species. Using the atomic coordinates from the RC crystal structure[4] and assuming that the Q_Y transition dipoles are aligned along the nitrogens of ring I and III in the bacteriochlorophyll and bacteriopheophytin monomers, the angle between the Q_Y transitions of H_L and B_L is ∼56°, and the angle between the Q_Y transitions of H_M and B_M is ∼60°. Since the emission dipole of B upon direct excitation is rotated ∼17° from the absorption dipole moment, the anisotropy we measure is within the range consistent with energy transfer from ^{1}H to B followed by emission from ^{1}B. We conclude that the identity of the emitting state probed at 815 and 850 nm is ^{1}B and that the kinetics reflect the excited state dynamics of ^{1}B.

Time-Resolved ^{1}B Fluorescence Spectrum. Observations of ^{1}B bear on potential excited state pathways as well as on the mechanism of energy transfer in RCs. Jean et al. calculated that the rate constant of energy transfer from ^{1}B to P, according to the Förster mechanism, should be an order of magnitude slower than what is observed.[17] The rate constant for energy transfer between two pigments is proportional to the spectral overlap between donor emission and the acceptor absorption. Since the position of the ^{1}B emission band in the RC had not been measured, Jean et al. used the 190 cm^{-1} Stokes shift of isolated bacteriochlorophyll *a* in ether solution at room temperature,[18] placing the emission maximum at 815 nm. To reconcile the observed ultrafast kinetics and the small spectral overlap between ^{1}B emission and the dominant absorption of P ascribed to its lower exciton band (P_-), energy transfer to the upper exciton state of P (P_+) followed by fast (∼100 fs) internal conversion to P_- was proposed. Jean et al. placed the peak of the absorption of the upper exciton state at 815 nm, thereby maximizing overlap with the estimated ^{1}B emission, and the oscillator strength of P_+ was assumed to be one-fourth that of P_-.

The corrected amplitudes (see Experimental Section) of the time-resolved fluorescence between 800 and 825 nm following excitation of WT RCs at 760 nm are shown in Figure 5A. The emission is peaked at 805 nm. These results indicate that the Stokes shift of ^{1}B emission on the 100 fs time scale and at 85 K is nearly zero in WT RCs, substantially less than the values for monomer bacteriochlorophyll *a* in liquid[18] and frozen solutions.[19] In RCs that fold without incorporating the special pair, steady state fluorescence from ^{1}B exhibits a Stokes shift of ∼80 cm^{-1} at room temperature.[20,21] The lack of any appreciable Stokes shift in the WT protein indicates that energy transfer from ^{1}B to P happens before significant relaxation of the excited state of B. If the overlap of ^{1}B emission with the ground state to P_+ absorption is a significant factor in determining the rate of energy transfer from ^{1}B to P_-, as in the calculations of Jean et al., then the time-resolved fluorescence spectrum reported here indicates that the maximum rate of singlet energy transfer would be achieved only if the ground state to P_+ absorption occurs at 805 nm, not 815 nm.

The location of the absorption of the upper exciton state of the special pair in WT RCs has been the subject of much debate.[22−24] It is generally thought to overlap with the low energy shoulder of the B band. Most data in the literature are consistent with B_L absorption at higher energy and B_M at lower energy, with the latter contributing most of the intensity to the shoulder around 810 nm.[22,25−28] This partitioning of intensity in the 800 nm band is strongly supported by the absorption changes in the M182HL mutant where the low energy shoulder is absent and a new, reasonably well-resolved band appears on the high energy side[29] (Figure 2). Furthermore, in the M182HL mutant, the low energy side of the B band is unstructured, providing no evidence for an absorption feature that might be assigned to P_+. Photochemical hole burning studies on WT at 4.2 K,[30,31] photon echo excitation spectra of R26 RCs at 77 K,[32] and linear dichroism measurements on WT at 10 K[27] show features centered at 811, 813, and 810 nm, respectively, which have been assigned to P_+. On the basis of these assignments, one would expect to see a structured absorption band in this region of the spectrum in the M182HL mutant, but no such feature is apparent. Therefore, if there is a ground state to P_+ absorption band in this region of the spectrum with appreciable oscillator strength, then it must be under B_L and peaked close to 805 nm. Such a peak position would maximize overlap with ^{1}B emission, thereby maximizing the rate of energy transfer from ^{1}B to P_+, as mentioned above.

Recent work from Scherer and co-workers[24] has addressed the mechanism of energy transfer in R26 RCs at room temperature. Their pump−probe data identify an absorption feature centered at 825 nm and show rapid spectral changes around 800 nm that are interpreted as a 260 cm^{-1} red shift of ^{1}B over 20 fs. The 825 nm band is assigned to P_+ and, as for Jean et al.,[17] the red shift of ^{1}B is necessary to achieve sufficient spectral overlap with a ground state to P_+ absorption. The spectral shift they observe contrasts with the time-resolved emission spectrum presented here for WT RCs at 85 K, which shows essentially no Stokes shift on the 100 fs time scale. If $^1B \rightarrow P_+$ energy transfer is important in feeding energy to P_-, the diminished spectral overlap between ^{1}B emission and a ground state to P_+ absorption centered at 825 nm would result in a slower energy transfer lifetime than is observed. It is possible that a Förster-type mechanism is inadequate to describe energy transfer from ^{1}B to P_+, that Scherer and co-workers misinterpreted the rapid spectral changes in the B band region, or both. Data from the M182HL mutant presented below support the hypothesis that a Förster-type mechanism is insufficient.

Energy Transfer Kinetics in the M182HL Mutant Compared to WT. In WT, the B_L and B_M bands are not well resolved, making independent measurement of the singlet excited state lifetimes of ^1B_L and ^1B_M difficult. Presumably, the fluorescence at all wavelengths between 800 and 850 nm has contributions from both ^1B_L and ^1B_M, since the B_L and B_M absorption bands overlap significantly and the emission spectrum (Figure 5A) is similarly unresolved. Because the decay kinetics at all wavelengths are the same and are essentially monoexponential, within experimental error, it appears that the excited state dynamics of ^1B_L and ^1B_M are similar, if not the same. The separation of the B_L and θ_M absorption bands in the M182HL mutant RC (Figure 2B) provides an opportunity to probe the excited state dynamics of the individual accessory chromophores in the B binding sites. Again the decay kinetics at all wavelengths between 790 and 820 nm for excitation at 750 nm are the same and are essentially monoexponential, within experimental error. This suggests that the decay of the singlet excited state of the monomer bacteriopheophytin, $^1\theta_M$, is similar to that of the monomer bacteriochlorophyll, ^1B_L. Furthermore, for excitation in the H band, the M182HL mutant exhibits similar energy transfer kinetics, measured both for the emission near the B band and for the rise of emission of ^{1}P at 920 nm, as for WT RCs.

Measurements of ^{1}B lifetimes may be useful for studying alternate charge separation pathways such as $^1B_L \rightarrow B_L^+H_L^-$

or $^1B_L \rightarrow P^+B_L^-$. There is no consensus on the rate constants of these events. Using resonance higher-order Stark spectroscopy, we have measured a several ps or longer time constant for $^1B_L \rightarrow B_L^+H_L^-$ in WT[33,34] and in the M182HL mutant.[35] Van Brederode et al. interpret their transient absorption results in WT as $^1B_L \rightarrow P^+B_L^-$ competing with $^1B_L \rightarrow P$, each with a 360 fs lifetime.[36] Free of the complications associated with transient absorption measurements in the RC, such as overlapping absorption bands and transient electrochromic bandshifts, fluorescence lifetime measurements probe the excited state dynamics directly. In the M182HL mutant, one can observe the dynamics of ^1B_L or $^1\theta_M$ independently. If the scheme proposed by van Brederode et al. were correct, one would expect to measure decay lifetimes of 360 fs for $^1\theta_M$ and 180 fs for ^1B_L; however, we see no differences in the lifetimes along the L and M branches in this mutant or in WT, where wavelength-independent kinetics are observed. Further discrepancies will be discussed in part 4 of this series.[9]

Time-Resolved Emission Spectrum of the M182HL Mutant Compared to WT. The corrected amplitudes of the time-resolved fluorescence decays between 790 and 820 nm are shown in Figure 5B for the M182HL mutant. The time-resolved emission spectrum is considerably broader than for WT with a peak at 805 nm and a noticeable shoulder around 797 nm. To avoid overwhelming background problems, the sample must be excited at 750 nm in order to observe emission at 790 nm (see Experimental Section). H_M is excited relatively more than H_L at 750 nm, so one might expect to see more emission at 797 nm than at 805 nm; however, the relative amplitudes are about the same. This can be rationalized by the greater oscillator strength of B_L (compared with θ_M) giving rise to more emission from ^1B_L than from $^1\theta_M$. The results suggest that the Stokes shift for θ_M is 70−100 cm^{-1} and for B_L is ∼35 cm^{-1}. The Stokes shift for monomer bacteriopheophytin *a* in the B_M binding site is close to the value of 120 cm^{-1} measured at 77 K in (2-methyl)THF for isolated bacteriopheophytin.[19] It is interesting that the rate of energy transfer from $^1\theta_M$ to P is the same in this mutant as $^1B_{L,M}$ to P in WT. Even with the 70−100 cm^{-1} Stokes shift for θ_M emission, one would expect substantially different spectral overlap with whatever feature of the P band absorption is responsible for energy transfer in a Förster-type analysis. In this case, the observed energy transfer lifetime for $^1\theta_M \rightarrow P$ would be different from $^1B_L \rightarrow P$ in this mutant and from $^1B_{L,M} \rightarrow P$ in WT, but it is not. This result is reminiscent of what was observed in the β mutant, M214LH, where replacement of the monomer bacteriopheophytin, H_L, with bacteriochlorophyll has little effect on the energy transfer rate constant measured by the rise of ^1P emission despite a substantial shift in absorption.[5] This further supports the hypothesis that singlet energy transfer is not predominantly occurring by a Förster dipole−dipole mechanism.[37] If the relative electronic interactions for energy transfer along the functional and nonfunctional sides is proportional to that for electron transfer between the same chromophores, then observations of energy transfer may be relevant to electron-transfer asymmetry.

In conclusion, the rise of spontaneous fluorescence peaked near the absorption maximum of the accessory bacteriochlorophylls is observed within 100 fs of excitation of the monomeric bacteriopheophytins. The time-resolved fluorescence anisotropy and kinetics suggest that the population is ^1B. This is the first report of ^1B emission in functional RCs and indicates that the mechanism of energy transfer from ^1H to P involves ^1B as a real intermediate. That is, the initially excited monomer bacteriopheophytins, $^1H_{L,M}$, transfer energy first to the accessory bacteriochlorophylls, creating $^1B_{L,M}$, which in turn transfer energy to the special pair. Furthermore, the time-resolved emission spectrum of the monomer bacteriochlorophylls shows that the Stokes shift is ∼0 cm^{-1}, which has implications for the position of the upper exciton band of P in singlet energy transfer models where P_+ facilitates fast energy transfer from ^1B to P_-.

Acknowledgment. This work was supported in part by a grant from the NSF Biophysics Program. The fluorescence upconversion facilities are supported by the Medical Free Electron Laser Program of the Office of Naval Research under Contract N00014-94-1-1024.

Appendix

Data Analysis for Sequential Energy Transfer. If energy transfer $^1H \rightarrow B$ occurs with rate constant k_1, $^1B \rightarrow P$ occurs with rate constant k_2, and ^1P undergoes electron transfer with rate constant k_3:

$$^1H \xrightarrow{k_1} {}^1B \xrightarrow{k_2} {}^1P \xrightarrow{k_3} P^+H^-$$

then the excited state dynamics of ^1P are described by

$$[^1P] = \frac{k_1k_2}{k_2-k_1}\left[\frac{1}{k_3-k_1}e^{-k_1t} - \frac{1}{k_3-k_2}e^{-k_2t} + \left(\frac{1}{k_3-k_2} - \frac{1}{k_3-k_1}\right)e^{-k_3t}\right] \quad \text{(A1)}$$

or as the more general model function used in fitting:

$$[^1P] = A_1e^{-k_1t} + A_2e^{-k_2t} + A_3e^{-k_3t} \quad \text{(A2)}$$

Thus, in general, the rate constants k_1, k_2, and k_3 appear in either the rise or decay of ^1P and must be accounted for in the fit to the data. In the RC the two energy transfer steps are roughly an order of magnitude faster than electron transfer, therefore $k_3 < k_1$ and k_2. Note that if $k_1 > k_2$, ^1P is expected to rise with k_2 and decay with k_1 and k_3, whereas if $k_1 < k_2$, ^1P is expected to rise with k_1 and decay with k_2 and k_3. Within the range of reasonable rate constants for the RC, the amplitudes of all three components are expected to be significant.

Figure 7 shows simulated data with Poisson-distributed noise fit to model functions with two and three exponential components along with the corresponding residuals. The rate constants used for $^1B \rightarrow P$, $(160\ fs)^{-1}$, and the decay of ^1P, $(1.2\ ps)^{-1}$, were measured independently by exciting B and monitoring the rise and decay of emission from ^1P.[5] In each simulation, the rate constant of $^1H \rightarrow B$ was varied. A Gaussian cross correlation with fwhm of 150 fs (as in our experiments) was used for convolution with the model function (A2). The residuals of the two-component fit exhibit structure characteristic of an inaccurate fit of the rise and peak of the fluorescence. It is seen that only when the lifetime of $^1H \rightarrow B$ becomes significantly less than the fwhm of the cross correlation, does the need for adding a third component diminish due to poor resolution.

Since ^1P decay exhibits heterogeneous kinetics,[38−40] the experimental data require a fourth component with a lifetime of many picoseconds whose amplitude is small (a few percent) compared to the other components. A typical data set for WT RCs exciting at 760 nm and monitoring emission at 920 is

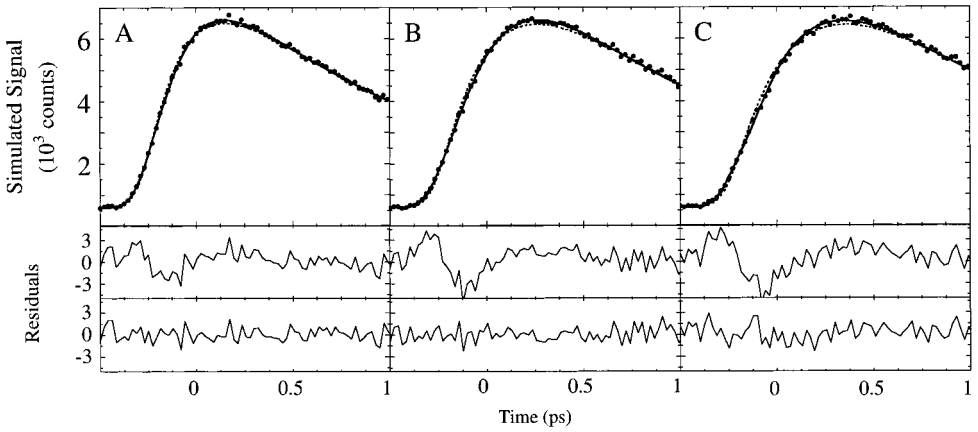

Figure 7. Simulated data with Poisson-distributed noise for excitation of H and emission from P. The rate constant of ^{1}B → P was fixed to (160 fs)$^{-1}$, the decay of ^{1}P fixed at (1.2 ps)$^{-1}$, and the rate constant of ^{1}H → B set to (A) (80 fs)$^{-1}$, (B) (160 fs)$^{-1}$, and (C) (240 fs)$^{-1}$. A Gaussian cross correlation with fwhm of 150 fs was used for convolution with the model function. The resulting two-component fit (dashed) and three-component fit (solid) are overlayed with the simulated data. The residuals of the two-component fits (middle panels) and three-component fits (lower panels) are shown. Parameters for the fits are listed in Table 2.

TABLE 2: Fits to Simulations with the Rate Constant of ^{1}B → P Fixed to (160 fs)$^{-1}$, the Decay of ^{1}P Fixed at (1.2 ps)$^{-1}$, and the Rate Constant of ^{1}H → B Varied[a]

^{1}H → B τ (fs)	no. of fit components	amp (%)[b]	τ (fs)	χ^2
80	2	−97	205	1.35
		100	1170	
	3	−87	165	0.98
		30	1190	
		69	54	
160	2	−98	288	2.08
		100	1130	
	3	−96	205	0.96
		39	99	
		61	1190	
240	2	−98	383	2.31
		100	1100	
	3	−99	257	1.03
		45	144	
		55	1190	

[a] A Gaussian cross correlation with fwhm of 150 fs was used for convolution with the model function. Values are the averages from three simulations. [b] Negative amplitudes indicate a rise component, while positive amplitudes indicate a decay component.

shown in Figure 6 along with fits using both three and four exponential components. The need for a fourth component is evident from the structured residuals of the three-component fit.

The 280 fs lifetime of the rise in the two-component fit to the simulated data in panel B of Figure 7 (Table 2) matches the rise time of ^{1}P emission when only three components are used to fit the experimental data. It was based upon this exact analysis, varying the rate constant of energy transfer from ^{1}H to B, that Stanley et al. arrived at the (160 fs)$^{-1}$ rate constant for singlet energy transfer from ^{1}H to B. The residuals from this analysis showed the characteristic pattern associated with fitting simulations for a three state model with only two components. A more accurate fit of both the simulations and the experimental data is obtained with an additional component, the justification for which is manifest in the equation describing the excited state dynamics of P (A1). Inclusion of this component permits us to more accurately determine the rate constant of ^{1}H to B, and comparison of the experimental data with the simulation fit values in Table 2 indicate that the lifetime is between 80 and 160 fs.

References and Notes

(1) Breton, J.; Martin, J.-L.; Migus, A.; Antonetti, A.; Orszag, A. *Proc. Natl. Acad. Sci. U.S.A.* **1986**, *83*, 5121−5125.

(2) Breton, J.; Martin, J.-L.; Fleming, G. R.; Lambry, J.-C. *Biochemistry* **1988**, *27*, 8276−8284.

(3) Jia, Y.; Jonas, D. M.; Joo, T.; Nagasawa, Y.; Lang, M. J.; Fleming, G. R. *J. Phys. Chem.* **1995**, *99*, 6263−6266.

(4) Deisenhofer, J.; Epp, O.; Sinning, I.; Michel, H. *J. Mol. Biol.* **1995**, *246*, 429−457.

(5) Stanley, R. J.; King, B. A.; Boxer, S. G. *J. Phys. Chem.* **1996**, *100*, 12052−12059.

(6) Schenck, C. C.; Gaul, D.; Steffen, M.; Boxer, S. G.; McDowell, L.; Kirmaier, C.; Holten, D. In *Reaction Centers of Photosynthetic Bacteria*; Michel-Beyerle, M. E., Ed.; Springer-Verlag: Berlin Heidelberg, 1990; Vol. 6, pp 229−238.

(7) Kirmaier, C.; Gaul, D.; Debey, R.; Holten, D.; Schenck, C. C. *Science* **1991**, *251*, 922−926.

(8) King, B. A.; Stanley, R. J.; Boxer, S. G. *J. Phys. Chem. B* **1997**, *101*, 3644−3648.

(9) King, B. A.; de Winter, A.; McAnaney, T. B.; Boxer, S. G. *J. Phys. Chem.*, submitted.

(10) Stanley, R. J.; Boxer, S. G. *J. Phys. Chem.* **1995**, *99*, 859−863.

(11) Goldsmith, J. O.; Boxer, S. G. *Biochim. Biophys. Acta* **1996**, *1276*, 171−175.

(12) Katilius, E.; Turanchik, T.; Lin, S.; Taguchi, A. K. W.; Woodbury, N. W. *J. Phys. Chem. B* **1999**, *103*, 7386-7389.

(13) We have previously demonstrated that the θ_M chromophore in M182HL raises the activation energy for triplet energy transfer from ^{3}P to the carotenoid, resulting in essentially no triplet energy transfer to the carotenoid at 85 K (deWinter, A.; Boxer, S. G. *J. Phys. Chem. B* **1999**, *103*, 8786−8789). One potential complication of this is that some fraction of excited RCs become trapped in the relatively long-lived ^{3}P state (∼100 μs lifetime) and do not return to the ground state in time to be excited by the next laser pulse 12 ns later (the excitation pulses are weak so only a small fraction of the sample is excited with each pulse). However, we are able to measure fluorescence from ^{1}P in the M182HL sample. Interestingly, there is no evidence of multiple ^{1}B decay components that might be expected if some RCs contain ground state P and others ^{3}P. The fluorescence dynamics of ^{1}B in RCs containing ^{3}P and P$^+$ will be described in part 5 of this series.

(14) The signal-to-noise of the data reported here is very good. As shown in the Appendix, it should be possible to resolve in the kinetics of ^{1}P the rate constants for each energy transfer step preceding the arrival of energy at P. This is what we have done by fitting the rise and decay of ^{1}P with four exponential components. We note, however, that fitting with three exponential components does not change the conclusions of this work.

(15) As described in the Appendix, for the two-step energy transfer model, the rate constant of each step appears in the dynamics of the final energy acceptor unless one of the rates is substantially faster than the cross correlation of the experiment. Unstructured residuals and reduced χ^2 for the three-component fit indicate that either ^{1}B transfers energy directly to P or, if an intermediate (I) exists in the energy transfer pathway ^{1}B → P (such as the upper exciton state of P, P$_+$), the lifetime of energy transfer from ^{1}I to P is faster than ∼60 fs and is therefore not detectable in the

dynamics of P. Scherer and co-workers (Arnett, D. C.; Moser, C. C.; Dutton, P. L.; Scherer, N. F. *J. Phys. Chem. B* **1999**, *103*, 2014−2032) and Martin and co-workers (Vos, M. H.; Breton, J.; Martin, J.-L *J. Phys. Chem. B* **1997**, *101*, 9820−9832) measure lifetimes of 65 fs and 50−100 fs, respectively, for $^1B \rightarrow P_+$, while Fleming and co-workers (Jonas, D. M.; Lang, M. J.; Nagasawa, Y.; Joo, T.; Fleming, G. R. *J. Phys. Chem.* **1996**, *100*, 12660−12673) measure a lifetime of 150 fs. According to our measurements, only the shortest of these reported lifetimes is possible.

(16) Ebrey, T. G.; Clayton, R. K. *Photochem. Photobiol.* **1969**, *10*, 109−117.

(17) Jean, J. M.; Chan, C.-K.; Fleming, G. R. *Isr. J. Chem.* **1988**, *28*, 169−176.

(18) Connolly, J. S.; Samuel, E. B.; Janzen, A. F. *Photochem. Photobiol.* **1982**, *36*, 565−574.

(19) Takiff, L.; Boxer, S. G. *J. Am. Chem. Soc.* **1988**, *110*, 4425−4426.

(20) Jackson, J. A.; Lin, S.; Taguchi, A. K. W.; Williams, J. C.; Allen, J. P.; Woodbury, N. W. *J. Phys. Chem. B* **1997**, *101*, 5747−5754.

(21) Moore, L. J. Ph.D. Thesis.

(22) Breton, J. *Biochim. Biophys. Acta* **1985**, *810*, 235−245.

(23) Reddy, N. R. S.; Kolaczkowski, S. V.; Small, G. J. *Science* **1993**, *260*, 68−71.

(24) Arnett, D. C.; Moser, C. C.; Dutton, P. L.; Scherer, N. F. *J. Phys. Chem. B* **1999**, *103*, 2014−2032.

(25) Vermeglio, A.; Clayton, R. K. *Biochim. Biophys. Acta* **1976**, *449*, 500−515.

(26) Knapp, E. W.; Fischer, S. F.; Zinth, W.; Sander, M.; Kaiser, W.; Deisenhofer, J.; Michel, H. *Proc. Natl. Acad. Sci. U.S.A.* **1985**, *82*, 8463−8467.

(27) Breton, J. In *The Photosynthetic Bacterial Reaction Center- - Structure and Dynamics*; Breton, J., Vermeglio, A., Eds.; Plenum: New York, 1988; Vol. 149, pp 59−69.

(28) Xie, X.; Simon, J. D. *Biochim. Biophys. Acta* **1991**, *1057*, 131−139.

(29) deWinter, A.; Boxer, S. G. *J. Phys. Chem. B* **1999**, *103*, 8786−8789.

(30) Johnson, S. G.; Tang, D.; Jankowiak, R.; Hayes, J. M.; Small, G. J.; Tiede, D. M. *J. Phys. Chem.* **1989**, *93*, 5953−5957.

(31) Raja, N.; Reddy, S.; Lyle, P. A.; Small, G. J. *Photosynthesis Res.* **1992**, *31*, 167−194.

(32) Meech, S. R.; Hoff, A. J.; Wiersma, D. A. *Proc. Natl. Acad. Sci. U.S.A.* **1986**, *83*, 9464−9468.

(33) Zhou, H. L.; Boxer, S. G. *J. Phys. Chem. B* **1998**, *102*, 9139−9147.

(34) Zhou, H. L.; Boxer, S. G. *J. Phys. Chem. B* **1998**, *102*, 9148−9160.

(35) Treynor, T.; Zhou, H. L.; Boxer, S. G. Manuscript in preparation.

(36) van Brederode, M. E.; van Mourik, F.; van Stokkum, I. H. M.; Jones, M. R.; van Grondelle, R. *Proc. Natl. Acad. Sci. U.S.A.* **1999**, *96*, 2054−2059.

(37) Förster, J. T. *Z. Naturforsch.* **1949**, *4a*, 321.

(38) Du, M.; Rosenthal, S. J.; Xie, X.; DiMagno, T. J.; Schmidt, M.; Hanson, D. K.; Schiffer, M.; Norris, J. R.; Fleming, G. R. *Proc. Natl. Acad. Sci. U.S.A.* **1992**, *89*, 8517−8521.

(39) Hamm, P.; Gray, K. A.; Oesterhelt, D.; Feick, R.; Scheer, H.; Zinth, W. *Biochim. Biophys. Acta* **1993**, *1142*, 99−105.

(40) Woodbury, N. W.; Peloquin, J. M.; Alden, R. G.; Lin, X.; Lin, S.; Taguchi, A. K. W.; Williams, J. C.; Allen, J. P. *Biochemistry* **1994**, *33*, 8101−8112.